Comprehensive study of supported PVDF membrane ageing in MBR: A direct comparison between changes at bench scale and full scale

Marcos Oliveira, Romain Mailler, Vincent Rocher, Yannick Fayolle, Christel Causserand

Comprehensive study of supported PVDF membrane ageing in MBR: a direct comparison between changes at bench scale and full scale

OLIVEIRA FILHO, Marcos[1]; MAILLER, Romain[2]; ROCHER, Vincent[2]; FAYOLLE, Yannick[3]; CAUSSERAND, Christel[1]

[1] Laboratoire de Génie Chimique, Université de Toulouse, CNRS, INPT, UPS, Toulouse, France

[2] SIAAP, Direction Innovation, 92700, Colombes, France

[3]Université Paris-Saclay, INRAE, PROSE, 92761, Antony, France

Corresponding author: OLIVEIRA FILHO, Marcos

E-mail: marcos.oliveira@siaap.fr

Phone: +33 1 41 19 52 12

Postal address : 82 Avenue Kléber, 92700 Colombes

Abstract

While membrane bioreactors (MBR) have been broadly applied to wastewater treatment, membrane ageing studies have focused mainly on: (i) understanding the chemical action of sodium hypochlorite or (ii) monitoring ageing in direct filtration facilities (drinking water, groundwater, etc.). Thus, a comprehensive investigation under full-scale MBR operating conditions is still required. In the present study, polyvinylidene difluoride (PVDF) hollow fibers were sampled from a full-scale MBR in northern Paris during 7 years of operation. In addition, pristine membranes were aged at bench scale by single soaking in hypochlorite solution at a concentration and pH similar to MBR cleaning protocols. Both bench-scale- and full-scale-aged hollow fibers were characterized using similar analytical methods to assess the contributions of chemical action and operating conditions to the ageing process. At bench scale, membranes experienced no changes in mechanical resistance, but intrinsic permeability (i) first increased as a result of the hydrophilic agent oxidation, i.e., polyvinyl pyrrolidone (PVP), increasing porosity with the appearance of small pores (diameter < 20 nm), and (ii) then the structure seemed to collapse and permeability decreased as a result. By contrast, membranes aged at full scale experienced a 46% decline in maximum tensile strength probably due to mechanical stress induced by aeration conditions in MBR. Besides, permeability increased for the whole period as a result of a more pronounced oxidation/dislodgement of PVP molecules leading to higher porosity and the appearance of bigger pores (diameter > 40 nm). These changes favored irreversible fouling in contrast to bench-scale ageing. Therefore, bench-scale ageing is not completely representative of full-scale ageing and membrane autopsies must be preferred to this end. However, permeability and PVP content measurements may be applied after cleaning as in situ nondestructive tools in full-scale MBR to monitor membrane ageing. Plant operators should be aware that a

continuous increase in intrinsic permeability may favor irreversible fouling accumulation demanding more frequent chemical cleanings.

Keywords: membrane bioreactor, ultrafiltration, hollow fiber, wastewater treatment, multiscale, long-term operation.

1. Introduction

Membrane bioreactors (MBR) have experienced an exponential growth during the past decade. The cumulative treatment capacity of large-scale facilities (>100,000 m^3/d), increased from 500,000 m^3/d in 2010 and is expected to reach over 14,000,000 m^3/d by 2025 [1]. The main drivers of this MBR expansion across the globe are stricter legislation concerning the reuse of the treated effluent, discharge to sensitive water bodies, space limitations, and retrofitting/upgrading wastewater treatment plants (WWTP) [2]. Membranes act as a reliable physical barrier, and thus MBR perform significantly better than classic processes. To illustrate, Bertanza et al. (2017) compared a full-scale MBR with a conventional activated sludge system (CAS) from a WWTP in Italy. Treating the same influent, MBR was able to remove 99.5% of chemical oxygen demand (COD) versus 90.6% for the CAS [3].

Despite the increasing interest in the application of MBR, membrane fouling is still a major concern. Several strategies are applied to reduce fouling such as aeration cycles, physical cleaning, i.e., relaxation or backwash, and chemical cleaning either by chemically enhanced backwash or cleaning-in-place (CIP) protocols [4]. However, these strategies may cause unrequired changes in membrane properties and are not able to eliminate fouling, instead residual fouling takes place over long-term use. The combined effect of residual fouling and changes in membrane properties in the long term results in membrane ageing, which is known

to hinder filtration capability and ultimately lead to membrane replacement [5]. Membrane lifespan is also a decisive factor in the economic efficiency of an MBR; a 19% reduction in the total costs of an installation was reported if membranes were replaced after 10 years instead of after 5 [6].

As a result, interest in understanding the ageing process of MBR has increased. Traditional studies focused on comprehending the changes in membrane properties due to exposure to chemicals often used in cleaning protocols, such as oxidants, bases, and acids. Among them, sodium hypochlorite (NaOCl) is the most commonly studied and widely used reagent in ultrafiltration processes thanks to its cleaning efficiency and associated low cost; unfortunately, however, NaOCl is also involved in the degradation of polymeric membranes. Polyvinylidene difluoride (PVDF), a chlorine-resistant polymer, has emerged as one of the most commonly used membrane materials for drinking water and wastewater treatment applications [7]. It has a high hydrophobic character and is usually mixed with hydrophilic and pore-forming additives, i.e., polyvinylpyrrolidone (PVP), polyethylene glycol (PEG), in the manufacturing of ultrafiltration membranes.

Since 2010, at least 22 studies have been published on PVDF membrane ageing. The main approach used in these studies was to accelerate ageing by single soaking in a hypochlorite solution and to observe the changes in membrane properties [8–21]. Generally, the chlorine exposure dose, which is the product ($C \times t$) between chlorine concentration (C) and soaking time (t), is used to monitor the ageing process. This parameter allows us to compare the ageing effects between bench scale and full scale. Other approaches included filtration of model fouling solutions and backwash hypochlorite cycles to include the impact of fouling [22–24]. Finally, one study investigated PVDF membrane ageing in full-scale direct filtration facilities [25].

The main conclusions drawn from these studies are: (i) the current understanding of PVDF membrane ageing is mainly based on chemical exposure at bench scale and (ii) contradictions can be found regarding permeability, pore size, and fouling reversibility changes with ageing, probably as a result of the differences in ageing conditions, in analytical methods, and in membrane type. Regarding these two points, the changes in PVDF membrane properties over time by direct filtration in drinking water facilities were elucidated in an initial study and the findings were later compared with changes observed in ageing of the same membranes at bench scale by single soaking and model fouling solution filtration/NaOCl backwash cycles [24,25]. By applying the same analytical methodology, the authors were able to conclude that single soaking is a reliable tool for predicting ageing changes in direct filtration facilities.

However, operating conditions in direct filtration and MBR are substantially different and a comprehensive study of changes in membrane properties over time under MBR operating conditions is still lacking. For direct filtration units, filtration cycles may take several hours at higher fluxes, i.e., over 30 $L.m^{-2}.h^{-1}$ (LMH) before backwash, due to a low-charged influent in terms of dissolved organic carbon (DOC), i.e., approximately 3.5 mgC/L [26]. For MBR, membranes are expected to handle much more polluted water (DOC over 100 mgC/L) with higher amounts of fouling agents and suspended solids, leading to smaller filtration fluxes (~25 LMH) and more frequent relaxation/backwash (every 10–90 min) [2]. In addition, one of the major differences between applications is membrane aeration, i.e., constant or intermittent aeration cycles to control cake formation. As membranes are potted without tension into the modules, this enables them to oscillate, which results in friction between membranes and limits cake deposition, whereas in direct filtration, aeration is not applied for this purpose as membranes are compacted in the module. To withstand these high shear stress conditions, the hollow fiber PVDF membranes are supported with more resistant polymers, such as poly-ethylene terephthalate (PET) [19].

The dynamics of filtration and fouling in MBR are expected to play a major role in membrane ageing compared with direct filtration facilities. In the only study dealing with membrane ageing in full-scale MBR, membrane end-life was triggered by the decline in filtration capacity (or increase in operating pressure) instead of by the maximum chlorine exposure advised by membrane manufacturers; however, no membrane characterization was performed to identify changes in the physical–chemical properties and to quantify the accumulation of residual fouling [5]

Thus, the aim of this study is to better understand PVDF membrane ageing in full-scale MBR under long-term operating conditions. To assess separately the chemical contribution due to NaOCl exposure, new membranes from the same brand were single soaked in NaOCl solution at bench scale and the changes in membrane properties were compared with full-scale ageing via regular membrane sampling in a WWTP over a 7-year period. To the best of the authors' knowledge, this is the first study to present an autopsy characterization of PVDF membranes harvested from a full-scale MBR for such a long period.

2. Materials and methods

2.1. Materials and ageing procedure

2.1.1. Chemical ageing at bench scale

For this study, virgin ZeeWeed® 500D (SUEZ Water Treatment Solutions, France) membranes were sampled from virgin ultrafiltration modules produced in 2018 equivalent to those installed in the WWTP facility (see section 2.1.2). These are supported PVDF hollow fibers with a nominal pore diameter of 0.04 µm.

Hypochlorite solutions used for the bench-scale ageing experiments were obtained by dilution of commercial sodium hypochlorite at 14 wt% (VWR chemicals, USA). In addition, concentrated sulfuric acid (analytical grade 95%, VWR chemicals, USA) for pH adjustment and sodium bisulfite (Honeywell Research Chemicals, USA) used for membrane storage were of analytical grade. Aqueous solutions were all prepared using pure water from Milli-Q^{TM} equipment (Thermo Fisher Scientific, USA).

Membranes were stored in 1 g/L sodium bisulfite solution at room temperature (21 ± 2 °C) before use. After rinsing in a large volume of pure water, laboratory ageing was performed by single soaking the pristine membranes in NaOCl solution at a total free chlorine concentration of 1000 ppm at room temperature; the intensity of ageing is presented as C × t ranging from 0 to 750,000 ppm.h. The volume of fibers did not exceed 1% of the soaking solution volume in order to avoid significant consumption of chlorine. Total chlorine concentration was checked three times a week via silver nitrate titration (Hach, USA). When a deviation of more than 10% from the target concentration was measured, the concentration was corrected by adding NaOCl. Concentrated sulfuric acid was added to adjust the pH to 9.0 and was corrected whenever changes greater than 5% were observed over time. These conditions are usually found in MBR applied to municipal wastewater treatment, and are equivalent to those applied to the MBR facility considered in this study (see 2.1.2). The actual free chlorine concentrations and pH measured during the bench-scale ageing ranged from 950 to 1060 mg Cl/L (ppm) and from 8.98 to 9.09, respectively; thus, the conditions were considered to be very stable.

In addition, membranes were also soaked in solutions of sulfuric acid and citric acid, separately, at pH 2.7, but no changes in membrane physical-chemical properties were observed. Thus, only the effects of sodium hypochlorite are analyzed in the present study.

2.1.2. Full-scale ageing

Membranes in the full-scale operation were sampled over 7 years from the Seine-Morée WWTP in France (SIAAP). This facility was commissioned in 2014 and treats 50,000 m^3/d wastewater (300,000-population equivalent) from the northern Paris urban area. This WWTP is composed of screening and grit and grease removal in its pretreatment unit, followed by a primary lamellar settler. The biological treatment and post-clarification are performed by MBR (Ultrafor®, Suez, France). Pretreated wastewater is divided equally into three biological basins (total volume of 39,500 m^3) composed of anaerobic, anoxic, and aerated zones. Then, the mixed liquor is sent to eight membrane tanks of 300 m^3 each. Each membrane tank contains 10 immerged cassettes composed of ZeeWeed® 500D membrane modules. The total filtering surface of this MBR is 106,000 m^2 (13,250 m^2 per tank).

Membranes are operated under coarse bubble aeration during 10-s on/off intervals. Filtration cycles occur for 15 min followed by physical cleaning, i.e., 30 s relaxation and 30 s backwash. Mixed liquor suspended solids concentration (MLSS) is controlled between 5 and 10 g/L by recirculation of mixed liquor from the membrane tanks to the biological basin and by sludge extraction periodically. Chemically enhanced backwashes (CEB) are performed once a week with NaOCl solution (200 ppm) and once every 2 weeks with citric acid solution (1000 ppm). Cleaning-in-place (CIP) is performed once a year. Ideally, membranes are submerged in a solution of 800 ppm NaOCl, and after rinsing they are then submerged in a solution of citric acid at a pH around 2.7. Each soaking is performed for 20 h with cyclic aeration every hour (giving a theoretical annual hypochlorite C × t of 16,000 ppm.h; however, deviations are not rare in full-scale operation). The influent and effluent characteristics along

with the precise membrane operating conditions are presented in the supplementary material (Table S. 1).

Membranes were sampled from the same two cassettes in the center of membrane tank 3 from 2016 to 2021 right before CIP (from 2 to 7 years in operation). Fibers were cut on both potted ends and stocked in sodium bisulfite solution at 1 g/L. Before characterization, membranes were cleaned at bench scale according to the CIP protocol applied at full scale. The C × t value for each sample is calculated using the concentration and exposure time given by the operators for each CIP. The C × t ascertained in the laboratory before measurements was also added to these values. The C × t value related to CEB was found to be negligible (500 ppm.h annually) and only the C × t related to CIP was considered. The C × t values of each sample are presented in Table 1.

Table 1: Exposure dose of study samples aged at bench scale and full scale.

Full scale		**Bench scale**
Operation time (months)	Estimated exposure dose C × t (ppm.h)	Exposure dose C × t (ppm.h)
		0
		12,000
		24,000
28	33,000	36,000
37	42,000	48,000
45	62,000	60,000
54	72,000	72,000
		78,000
		84,000
70	98,000	100,000
		125,000
		148,000

	170,000
	249,000
	500,000
	750,000

2.2. Characterization of membrane performance factors

Tensile tests

Tensile tests were performed on an INSTRON 3340 series apparatus (INSTRON®, USA). The initial distance between grips was fixed at 100 mm and samples of wet membranes were extended at a constant elongation rate of 110 $mm.min^{-1}$. Breaking force, elongation at break, and Young's modulus were calculated from the experimental stress–strain curves using Bluehill 3 software.

Filtration properties

Intrinsic membrane permeability was measured by filtration of pure water at different permeate fluxes (J) in KrosFlo Research apparatus (SpectrumLab, USA). Permeability was then calculated and corrected to 20°C according to Pellegrin et al. (2013) [27]. The values obtained for each sample (Lp) were then normalized with respect to the value of a pristine membrane (Lp_0) as the ratio Lp/Lp_0.

To assess fouling reversibility, 11-cm-long modules composed of three fibers were constructed and submitted to three successive cycles of filtration and backwash of mixed liquor sample. The mixed liquor was collected from the MBR recirculation channel and filtered at 1.2 µm on the same day. This suspension was stored at 4°C for a maximum of 2 weeks before use. The procedure was performed to avoid high variations in the mixed liquor characteristics over the storage time and to focus on colloidal fouling. The resulting matrix is

mainly composed of the colloidal fraction typically present in an MBR mixed liquor (COD: 15.6 ± 0.8 mg O_2/L; DOC: 7.3 ± 2.4 mg C/L). These experiments were conducted with a Convergence Inspector Hydra device (Convergence Industry, The Netherlands). In this assay, membranes were submitted to two cycles of 60-min filtration with this matrix at a fixed transmembrane pressure (TMP) of 0.55 bar and 30 min of permeate backwash at TMP 0.8 bar. The third filtration cycle was performed for 10 min prior to a final backwash of 30 min for practical reasons. Flowrate and pressure were automatically monitored every 2 s.

Membranes filtered pure water for 10 min prior to the mixed liquor filtration/backwash cycles at the same TMP, and pure water permeate flux (J_0) was measured. The permeate fluxes in mixed liquor (J) during filtration were then normalized by J_0, giving the curve J/J_0 presented in the supplementary material (Figure S. 1). Cleaning recovery after a backwash could then be expressed as a percentage of the initial normalized flux $(J/J_0)_{c1}$ according to Eq. 1. For instance, cleaning recovery presented in this study is obtained for the third filtration cycle $(J/J_0)_{c3}$. The cleaning recovery results allow us to estimate reversible fouling in terms of recovered filtration flux after backwash. The remaining non-recovered flux is related to the physically irreversible fouling fraction.

$$\text{Cleaning recovery (\%)} = \frac{(J/J_0)_{c1} - (J/J_0)_{c3}}{(J/J_0)_{c1}} \times 100\% \qquad \text{Eq. 1}$$

Evaluating how aged membranes would act when facing real fouling matrices (fouling propensity) is a key indicator to understanding the impact of ageing in a practical way. Some studies assessed these behaviors by using model solutions for filtration tests, usually composed of bovine serum albumin (BSA), sodium alginate, and/or polysaccharides to mimic real effluents [22,23]. Only one study performed tests with real mixed liquor, and although these matrices are not standardized, these protocols are expected to be more transposable to full-scale applications [8]. In the present study, both sets of samples (bench-scale- and full-

scale-aged membranes) were submitted to hydraulic cleaning recovery tests against foulants (mainly colloidal) from a real MBR mixed liquor in order to assess fouling reversibility.

2.3. Characterization of membrane physical–chemical properties

The physical–chemical properties of aged membranes were measured to identify the impact of NaOCl exposure at bench scale and the impact of operating conditions at full scale.

Infrared spectrometry

Functional chemical groups present on the membrane surface were analyzed via attenuated total reflection-Fourier transform infrared (ATR-FTIR) using a Nicolet iS5 spectrometer with a germanium cell (Thermo Fisher Scientific, USA). Infrared (IR) spectra were recorded at wavelengths from 600 cm^{-1} to 4000 cm^{-1} (128 scans at 4.0 cm^{-1}). Spectral analyses were performed with OMNIC® software. Changes in the 1674-cm^{-1} band (stretching vibration of carbonyl) were studied among other changes. This is a characteristic band associated with PVP used as hydrophilic agent by polymeric membrane manufacturers [28]. In order to normalize the values from each spectrum, PVP content was determined by the ratio between the intensity of the PVP peak (at 1674 cm^{-1}) and the band at 1403 cm^{-1}, related to C-F bonds from PVDF, known for its stability over sodium hypochlorite exposure [25]. In the present study, the PVP content of each aged sample is then expressed as a percentage of the value obtained for pristine membranes.

Surface hydrophobicity

Membrane surface hydrophobicity was characterized indirectly by contact angle measurements using the captive bubble method, which was previously described by Pellegrin et al. (2013). This method is used instead of the sessile drop technique in the case of porous

materials since it provides a more realistic measure as the membrane surface is kept in wet conditions [27]. For these measurements, PVDF surface skin from samples was first peeled off from the support material and fixed on a microscope slide, then immersed in the measuring cell filled with water. This method was only applied to bench-scale samples as peeling off did not allow us to recover a piece of intact skin from the full-scale samples, and measurements on the whole hollow fiber led to large errors due to their concave surface.

Pore size and volume

Pore volume and pore size distributions were measured by nitrogen adsorption for both bench-scale- and full-scale-aged samples. Membrane samples of 0.2 g were oven dried at 40 °C for 72 h and placed in the measurement chamber. Measurements were carried out at 77 K in a Belsorp apparatus (Microtrac MRN, Germany). The sorption isotherms can be used to determine pore volume and pore size distribution by the BJH model [29].

Microscopy

Scanning electron microscopy (SEM) was performed using a Hitachi TM3030. First, dried membranes were coated in 5 nm of gold. Then, images with an optical magnification of 60× and 500× were acquired in order to qualitatively evaluate the topographic aspects of the membranes.

2.4. Statistical analysis

Statistical analyses were conducted in R software [30]. In order to visualize the relationship among changes in membrane properties, a principal compound analysis (PCA) was performed for each samples from bench-scale and full-scale ageing. Then, linear correlations were tested

for all properties and p-values relate to the null hypothesis that one property remains stable despite the other. All analysis were performed at 95% confidence level.

3. Results

First, the changes in performance factors, namely, mechanical and filtration properties, are presented for both chemical ageing at bench scale and at full scale (section 3.1). Then, the physical–chemical properties are evaluated in order to establish cause–effect relationships (section 3.2). Finally, these changes due to sodium hypochlorite contact and MBR operating conditions are discussed further in sections 4.1 and 4.2, respectively.

3.1. Impact of ageing on membrane performance factors at bench scale and full scale

3.1.1. Mechanical properties

The changes in ultimate tensile strength for bench-scale and full-scale samples as a function of exposure dose are presented in Figure 1.

At bench scale, single soaking in sodium hypochlorite did not cause statistically significant changes in the ultimate tensile strength of ZeeWeed® membranes (Kruskal test, p = 0.468). This stability was also observed in percent elongation at break and Young's modulus (data not shown).

Regarding membranes aged at full scale, the ultimate tensile strength showed a 45% decline over the study time. Nevertheless, operators did not report significant fiber breakage during the whole operation period.

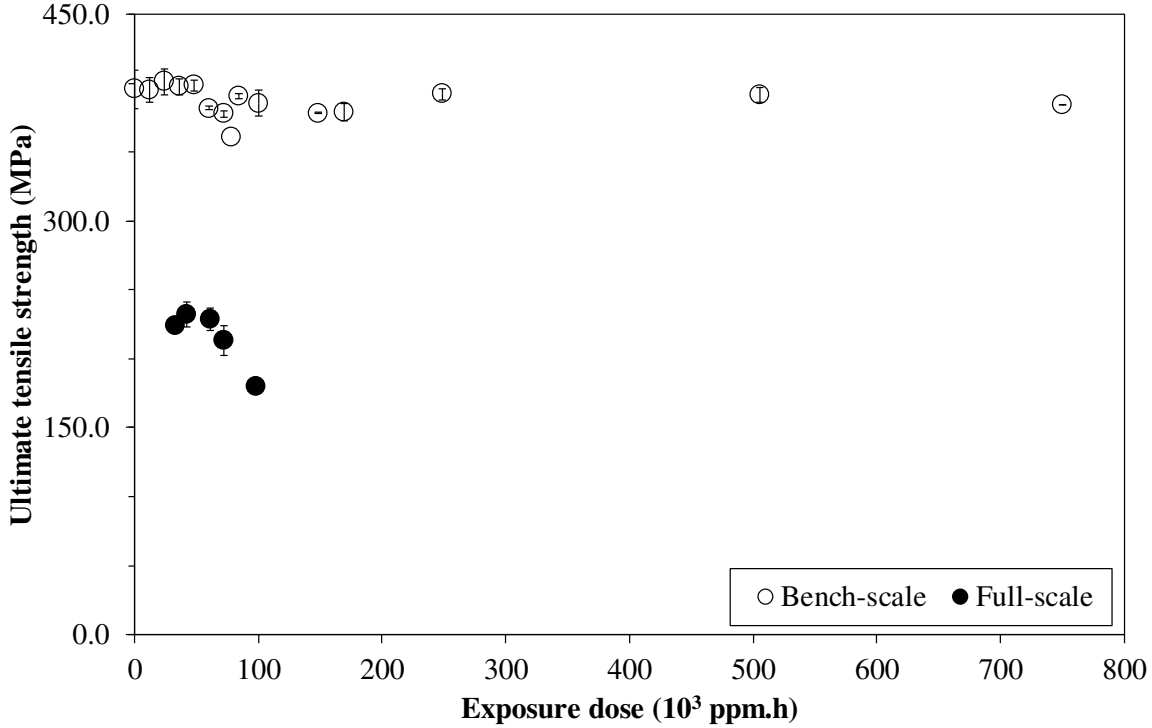

Figure 1: Ultimate tensile strength for bench-scale- and full-scale-aged membranes.

3.1.2. Filtration properties

3.1.2.1. Intrinsic membrane permeability

Intrinsic membrane permeability is presented in Figure 2 as a ratio between the values of aged and pristine membrane (Lp/Lp_0) with respect to $C \times t$.

For ageing at bench scale, these results can be divided into three phases. The first phase, corresponding to membranes exposed to a $C \times t$ of up to 78,000 ppm.h, showed an increasing trend until reaching 1.9 times the initial permeability. The second phase ($C \times t$ = 78,000 – 150,000 ppm.h) of decreasing Lp/Lp_0 showed an increase in $C \times t$; and in the third phase, after 150,000 ppm.h membranes reached a plateau at values comparable to a pristine membrane.

Moreover, the Lp/Lp_0 of membranes at full scale showed an increasing trend with C × t (and the associated time of operation), although to a lesser intensity than bench-scale-aged samples, at least during the 7 years of data collection in the present research.

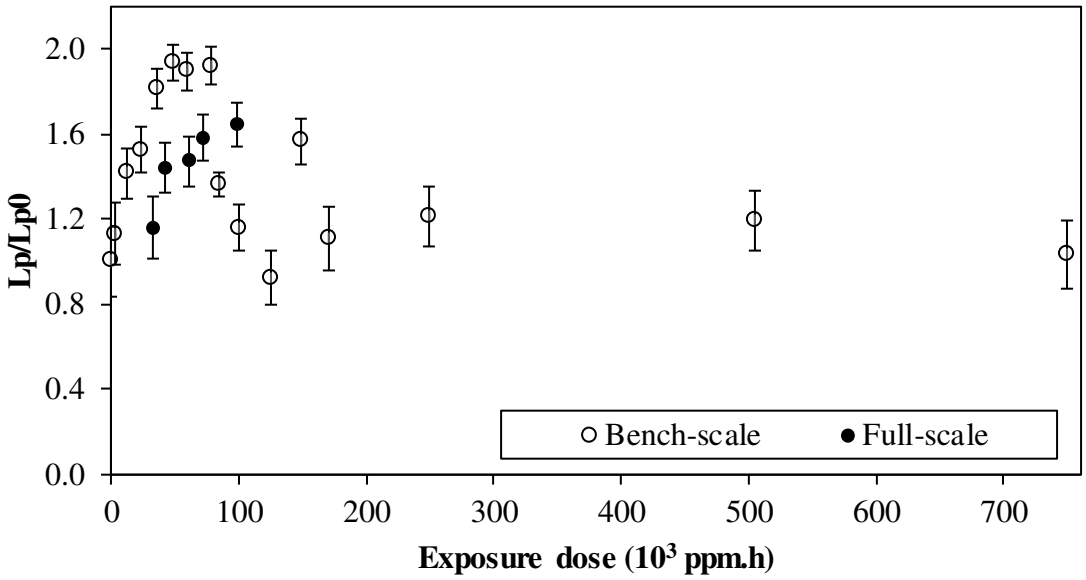

Figure 2: Changes in intrinsic permeability with respect to virgin membranes (Lp/Lp0 ratio) at bench-scale and full-scale ageing.

3.1.2.2. Mixed liquor fouling reversibility

Pristine membranes recovered 56% of their flux and samples aged up to 125,000 ppm.h reached 65%; subsequently, samples exposed to 500,000 ppm.h experienced a decline to a value of 51% (Figure 3). When comparing these values with those obtained for full-scale samples (Figure 3), we found that cleaning recovery was always higher in samples aged at bench scale, regardless of the C × t value. In addition, full-scale harvested membranes showed a decline from 39% to 32% in cleaning recovery when the C × t increased from 33,000 to 100,000 ppm.h.

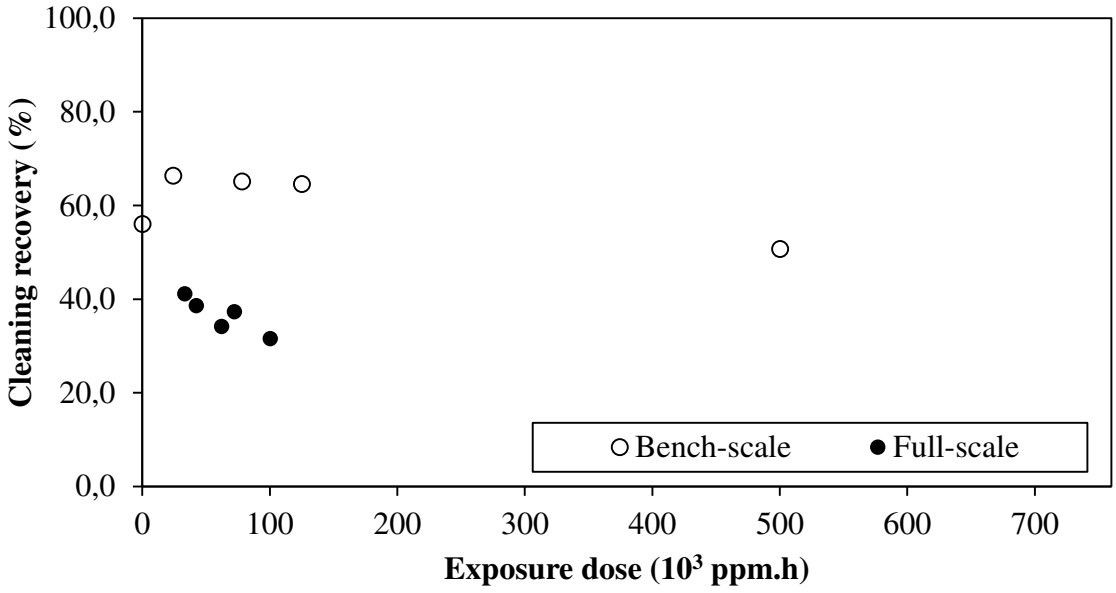

Figure 3: Cleaning recovery (%) after two cycles of filtration and hydraulic backwash on fibers aged at bench scale and at full scale.

3.2. Impact of ageing on membrane physical–chemical properties at bench scale and full scale

3.2.1. Membrane surface chemistry

PVP degradation

PVDF is a chlorine-resistant polymer and is relatively stable over long-term hypochlorite exposure. By contrast, PVP is generally highly reactive in alkali conditions or in the presence of oxidative radicals. The IR spectra presented in Figure 4.A confirmed the PVDF fingerprint stability over NaOCl exposure (wavelengths considered: 1403, 1277, 1178, 1072, 880, and 841 cm^{-1}). The band at 1674 cm^{-1} indicated the presence of a hydrophilic agent. This band is related to carbonyl stretches bonded to the amide group in the PVP chain. Moreover, it is known that the area between 1500 and 1800 cm^{-1} concentrates most of the PVP degradation products [28]. Therefore, this zone is enlarged in Figure 4.B and C for both bench-scale and full-scale ageing, respectively. The PVP content of aged membranes with respect to pristine

membranes among bench-scale- and full-scale-aged membranes as a function of C × t is presented in Figure 5. Both sets of membranes showed a decline in PVP content that can be associated with either its removal from the membrane structure and/or to its degradation into other by-products. However, no change in PVP content is observable above 78,000 ppm.h for bench-scale samples.

The decline in PVP content for full-scale-aged membranes seemed to follow the same trend observed at bench scale for C × t values lower than 78,000 ppm.h. For higher C × t values, the PVP content continued to decrease reaching 25% of the initial content (Figure 5).

(A)

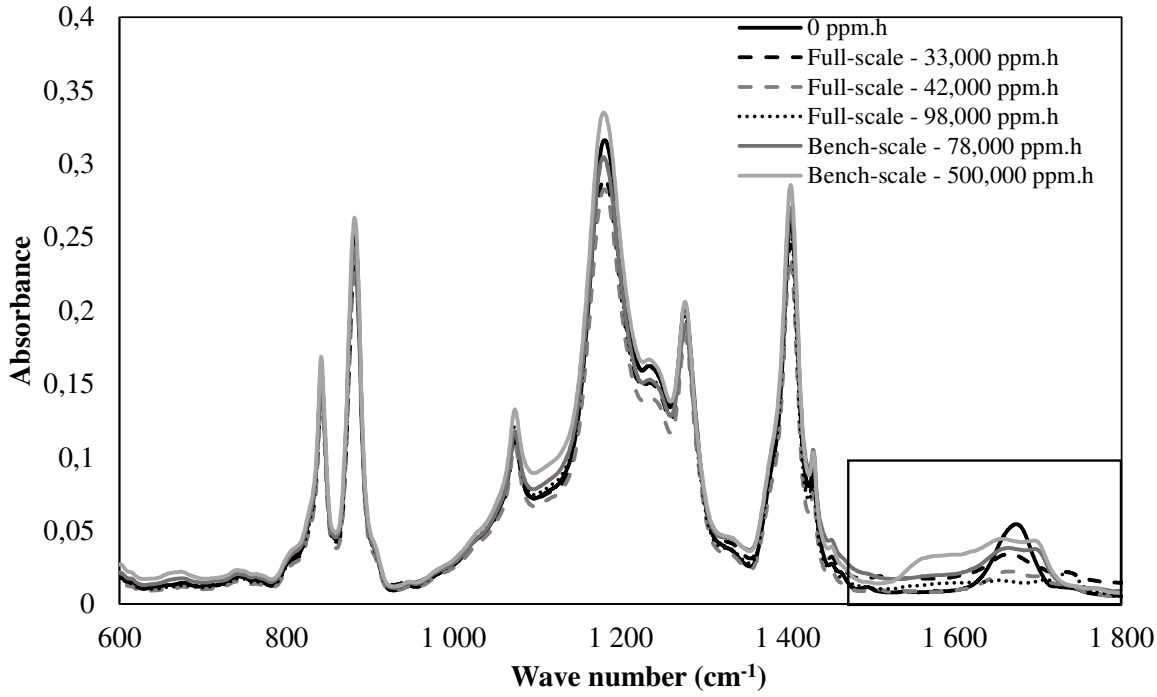
0,4
0,35
0,3
0,25
0,2
0,15
0,1
0,05
0
Absorbance
600
800
1 000
1 200
1 400
1 600
1 800
Wave number (cm-1)
0 ppm.h
Full-scale - 33,000 ppm.h
Full-scale - 42,000 ppm.h
Full-scale - 98,000 ppm.h
Bench-scale - 78,000 ppm.h
Bench-scale - 500,000 ppm.h

1

(B)

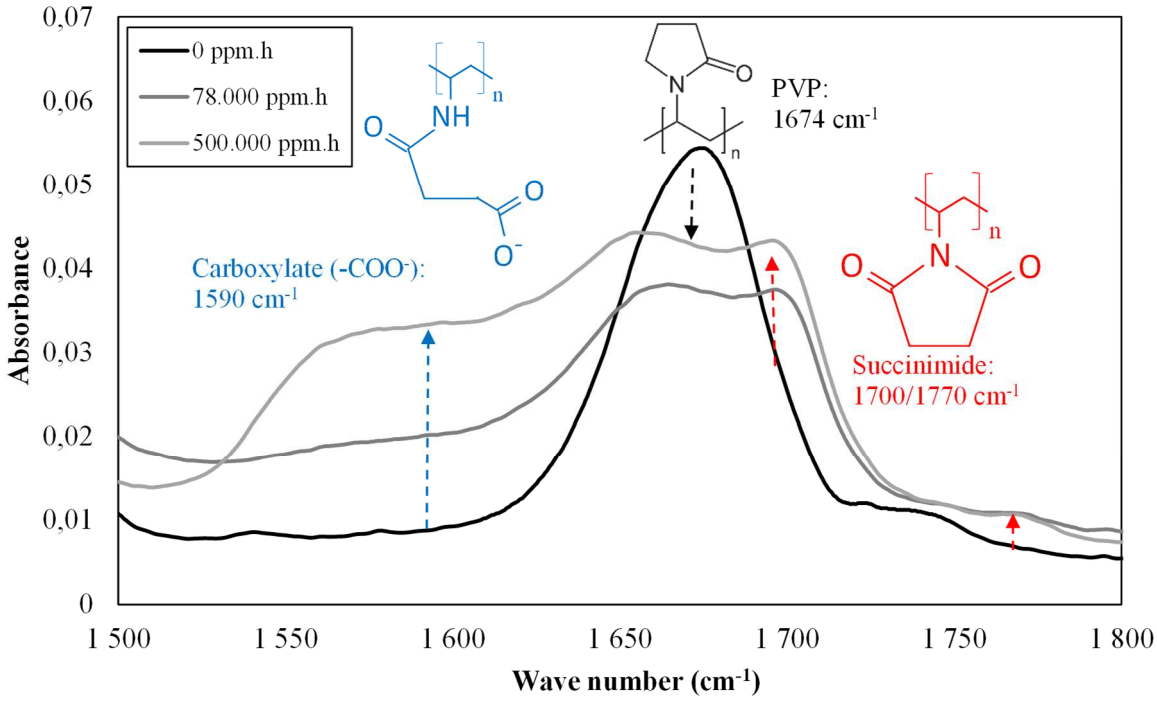
0,07
0,06
0,05
0,04
0,03
0,02
0,01
0
Absorbance
1 500
1 550
1 600
1 650
1 700
1 750
1 800
Wave number (cm-1)
0 ppm.h
78.000 ppm.h
500.000 ppm.h
PVP:
1674 cm-1
Carboxylate (-COO-):
1590 cm-1
Succinimide:
1700/1770 cm-1

2

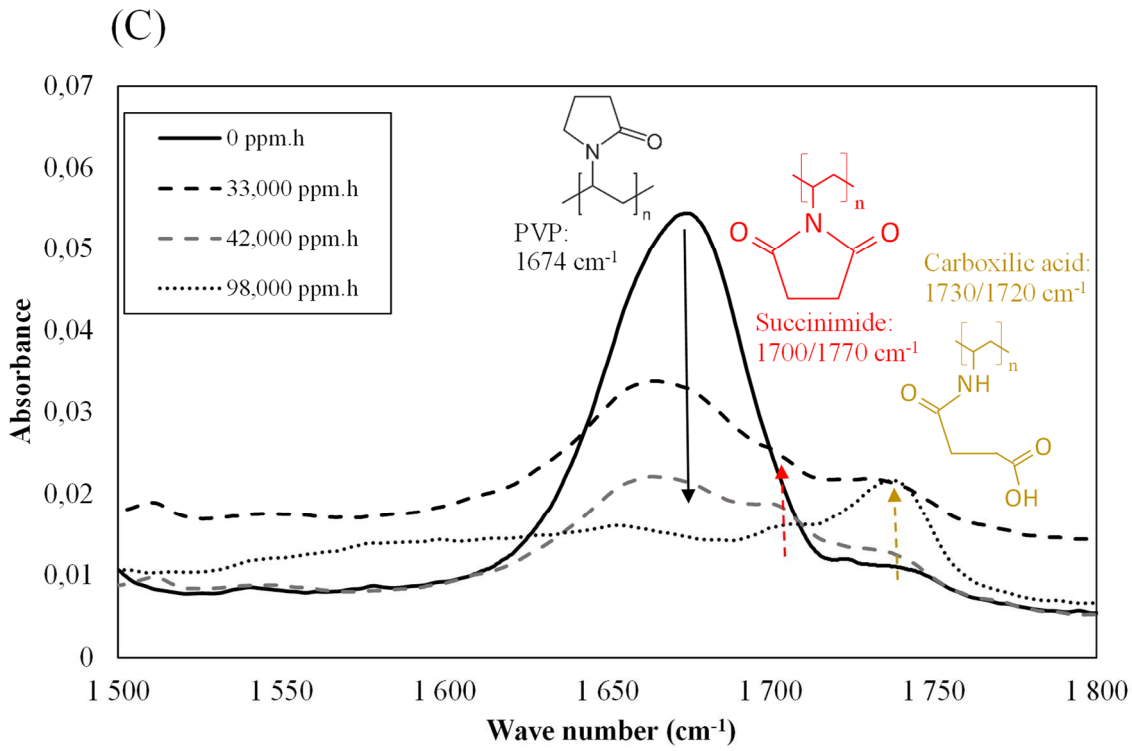

Figure 4: Full-range FTIR spectra (600–1800 cm^{-1}) of membranes aged at bench scale and full scale (A) and enlarged view of the characteristic region of PVP and its degradation products (1500–1800 cm^{-1}) for samples aged at bench scale (B) and at full scale (C).

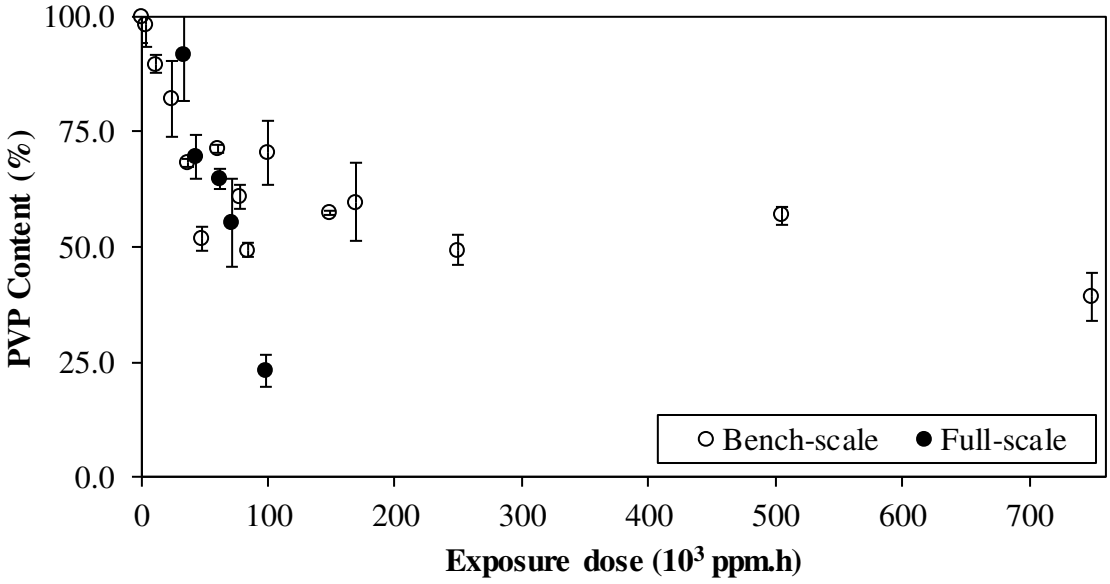

Figure 5: Change in PVP content at bench-scale and full-scale ageing as a function of the exposure dose.

Hydrophobicity

Chemical ageing at bench scale had no significant influence on the contact angles as all values ranged from 38.7 to 44.9° within the experimental errors (Kruskal–Wallis test, $p = 0.1041$). This result does not demonstrate that the membrane surface hydrophobicity is stable over hypochlorite exposure, but probably that the method is impacted by other phenomena (i.e., electrical charges).

Morphological properties

The results of pore volume as a function of pore diameter (dp) are presented in Figure 6 for membranes aged at bench scale (A) and at full scale (B). Regarding the pore volume of bench-scale ageing (Figure 6.A), an increase in porosity is noted up to 78,000 ppm.h, after which it seems that a collapse on the structure promoted an intense decline in pore volume for samples exposed to 125,000 and 500,000 ppm.h of hypochlorite. Moreover, these changes in total pore volume seem to be governed by an initial increase followed by a decline in the zone of small pores (dp < 20 nm, gray zone).

(A)

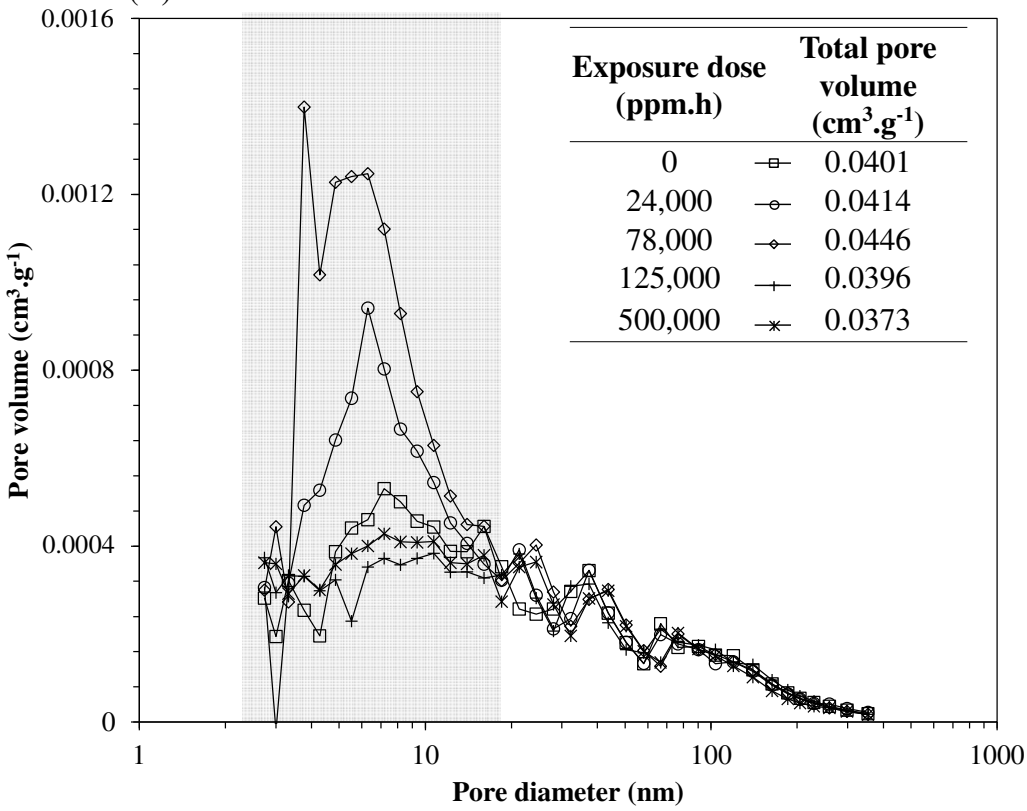
Exposure dose (ppm.h)
Total pore volume (cm3.g-1)
0 0.0401
24,000 0.0414
78,000 0.0446
125,000 0.0396
500,000 0.0373
Pore volume (cm3.g-1)
0.0016
0.0012
0.0008
0.0004
0
1
10
100
1000
Pore diameter (nm)

1

(B)

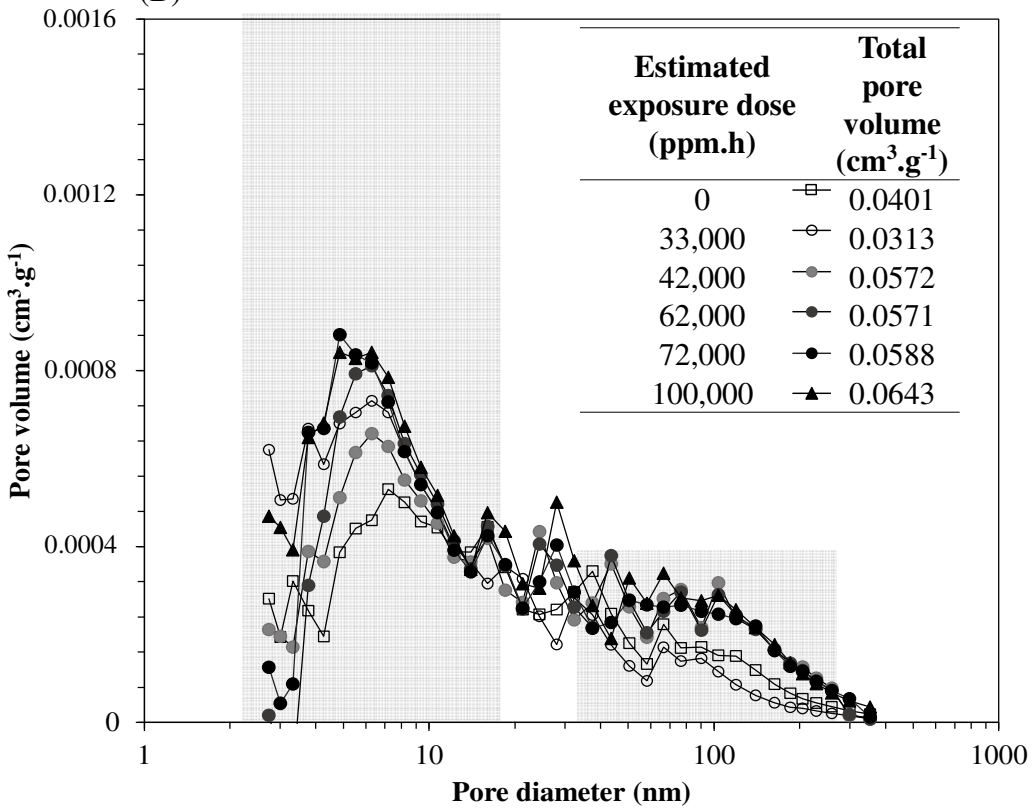
Estimated exposure dose (ppm.h)
Total pore volume (cm3.g-1)
0 0.0401
33,000 0.0313
42,000 0.0572
62,000 0.0571
72,000 0.0588
100,000 0.0643
Pore volume (cm3.g-1)
0.0016
0.0012
0.0008
0.0004
0
1
10
100
1000
Pore diameter (nm)

2

Figure 6: Pore volume and size distribution of chemically aged membranes at bench scale (A) and at full scale (B).

For membranes ageing at full scale (Figure 6.B), although samples harvested in the early phase of ageing (33,000 ppm.h) had a slightly lower porous volume, the same trend of an increasing number of small pores was observed. In addition, samples aged for 42,000 ppm.h showed an increasing number of larger pores (dp > 40 nm), reinforcing the notion that the ageing mechanisms at full-scale operation are not exactly the same as chemically aged samples at bench scale. These two zones are highlighted in gray in the graph in Figure 6.

SEM images were acquired and qualitatively confirmed the presence of these larger pores in full-scale-aged membranes (supplementary material – Figure S. 2). In addition, an increase in surface roughness can be observed when comparing full-scale- with bench-scale-aged and pristine samples.

4. Discussion

4.1. Sodium hypochlorite impact on membrane performance factors

Impact of NaOCl chemical ageing on mechanical resistance

In the case of supported membranes, mechanical resistance is mainly linked to the material used to support PVDF. By ATR-FTIR analysis, it was found that the supporting material of these membranes had 68% accordance with PET. PET is often used as a support material for ultrafiltration membranes. However, only few studies of membrane ageing characterized its mechanical resistance. Pulido et al. (2019) evaluated the properties of recycled PET-based membranes and concluded that the material was chlorine resistant after a 2-h exposure to a 5000-ppm solution [31]. However, the effects of long-term exposure were not determined. The results of bench-scale-aged samples in the present research indicate that the long-term

exposure to NaOCl does not impact the mechanical properties of these supported hollow fibers. Conversely, Wang et al. (2018) characterized hypochlorite aged membranes reinforced with PET nonwoven fabric and found a slight decline in ultimate tensile strength. It is worth noting that these membranes exhibited ultimate tensile strength in the range of 40 MPa, which is 10 times less resistant than fibers used in the present study.

Impact of NaOCl chemical ageing on intrinsic permeability

Changes in permeability of bench-scale-aged membranes can be associated mainly with: (i) changes in the surface physical–chemical characteristics, especially hydrophobicity and electrical charges and (ii) modifications in skin porosity. The first phase of increasing permeability between 0 and 78,000 ppm.h (Figure 2) was found to be linked to the decline in PVP content (Figure 5). Statistical analysis confirmed a significant correlation in this dose range, giving a correlation coefficient (r) of -0.951 (p = 0.0003, Pearson correlation test). Despite the decline in PVP, the contact angle values did not change significantly. However, changes in contact angle due to an increase in hydrophobicity may be counter-balanced by an increase in electrical surface charges, and this combined effect of the surface physical–chemical properties does not seem to significantly impact permeability [27].

Regarding the change in skin porosity, a formation of small pores (d_p < 20 nm) is observed in Figure 6.A, enhancing overall membrane porosity. In fact, FTIR spectra (Figure 4.B) showed that PVP molecules are not fully dislodged from the membrane structure. They are instead oxidized into succinimide (at 1700/1770 cm^{-1}) and carboxylates (1590 cm^{-1}) following the PVP degradation mechanism proposed by Prulho et al. (2013) [28]. These molecules remained (totally or partially) in the membrane structure, possibly leading only to the formation of small pores, whereas a full PVP dislodgement would lead to the formation of macro-voids. By contrast, there seems to be agreement in the literature that NaOCl exposure

causes PVDF membrane permeability to increase as a result of a pore enlargement due to the oxidation and dislodgement of PVP from the fiber structure [9,19,22,24]. However, Ravereau et al. (2016) similarly reported an increasing volume of pores smaller than 10 nm, only for PVDF membranes containing PVP when exposed to sodium hypochlorite, whereas PVDF membranes with no additive did not show any changes in pore size distribution [16].

After the exposure threshold of 78,000 ppm.h, the decline in Lp/Lp_0 was no longer correlated with PVP content. It seems that after the increasing porosity, the membrane structure collapsed ($C \times t > 78{,}000$ ppm.h), decreasing pore volume and Lp/Lp_0 as a result. Based on Gao et al. (2016), PVP is degraded into new products and macromolecular chains in the PVDF matrix may rearrange by crosslinking, which might be the reason for the shrinkage in porosity [23]. A statistically significant correlation was found between Lp/Lp_0 and the volume of smaller pores for the whole range of $C \times t$ studied ($r = 0.966$, $p = 0.008$, Pearson correlation test).

Impact of NaOCl chemical ageing on cleaning recovery

Cleaning recovery is also impacted by the physical–chemical properties of surface and porosity. Pore volume did not correlate well with cleaning recovery ($p > 0.05$), indicating that the appearance of small pores did not change the fouling mechanisms. Nevertheless, cleaning recovery is related to the interactions between foulants and membrane surface as well. Firstly, cleaning recovery increased with ageing, indicating that foulants became less attached to the membrane surface, i.e., increasing fouling reversibility. Irreversible fouling is mainly related to organic matter adsorption on the membrane surface, which is explained by the extended Derjaquin–Landau–Verwey–Overbeek (DLVO) theory as a synergic work of Van der Waals force, polar force, and electrostatic interactions. Foulants in mixed liquor are mostly hydrophobic organic matter and negatively charged at neutral pH [32]. When in contact with

NaOCl, the PVP cyclic group, pyrrolidone, is opened forming carboxylates. As a result, membranes may increase their negative charges as they age, leading to higher electrostatic repulsion between the membrane surface and foulants, enhancing then cleaning recovery. Recently, Li et al. (2021) confirmed the increase in negative charges as PVDF membranes aged in contact with NaOCl [12].

For further exposed samples (500,000 ppm.h), cleaning recovery dropped to 51%. We hypothesize that topographic changes (increase in roughness) may be playing a bigger role favoring foulant adsorption, as reported by Levitsky et al. (2011), and correlated well with an increase in protein adsorption onto the membrane surface [11].

4.2. Membrane ageing under MBR operating conditions at full scale

Full-scale operation effects on mechanical resistance

Regarding mechanical resistance, membranes aged by single soaking in hypochlorite solutions did not experience the weakening observed in the membranes at full-scale operation (Figure 1). These findings suggest that a synergic effect of aeration and filtration conditions in MBR may be the reason for the decline in ultimate tensile strength. However, the precise mechanism behind these changes could not be assessed and further studies are needed. Even though the functional groups showed no changes on the PET fingerprint (1124 and 1240 cm^{-1}) in the IR spectra (supplementary material – Figure S. 3), alterations in the support polymer crystalline structure, crosslinking/chain breakage, and material fatigue could be the reasons for this decline. This weakening could lead to fiber breakage, which could degrade the filtration quality. In addition, PVDF skin tearing was observed in SEM images of full-scale-aged samples (supplementary material – Figure S. 2 G and H) and can impact permeate

quality. Although FTIR spectra failed to confirm changes in the PVDF functional groups (Figure 4), other studies already reported embrittlement of PVDF due to dehydrofluorination and chain scission after exposure to NaOCl [15,16,22]. Nevertheless, operators reported no changes in the permeate quality over these 7 years of operation despite the decline in mechanical resistance.

PVP degradation differences between ageing at bench scale and full scale

The mechanisms of PVP degradation between bench-scale and full-scale ageing are also different (Figure 4.B and C, respectively). At bench scale, the sole effect of hypochlorite (pH 9.0) induces the production of carboxylate and succinimide from the chemical attacks to PVP molecules. These degradation products remained in the membrane structure. At full scale (Figure 4.C), the PVP peak (1674 cm^{-1}) is strongly suppressed and the typical peaks associated with by-products did not seem to increase to the same extent, with only a slight increase in the succinimide peak (1700 cm^{-1}) being observed, suggesting that PVP is oxidized into succinimide and then removed from the membrane structure. In addition, a peak at 1730 cm^{-1} (carboxylic acids) is formed, which can be assigned either to a PVP degradation product or to residual fouling. For the former, Prulho et al. (2013) reported that carboxylates (1590 cm^{-1}) are favored under alkali conditions, which is the case for the whole ageing process at bench scale [28]. At full scale, however, membranes are cleaned by sodium hypochlorite followed by citric acid solutions at a pH between 2.5 and 3.0, which might favor the formation of carboxylic acids versus carboxylates in the PVP degradation process. For the latter, it is worth noting that this carboxylic acid peak may also be assigned to residual fouling, as reported by Levitsky et al. (2011) [11].

Several studies compared PVP degradation in different ageing protocols. For instance, Causserand et al. (2015) found no significant differences in PVP degradation between single-

soaked membranes and performing filtration/backwash cycles in NaOCl solution at bench scale [33]. In addition, Robinson and Bérubé (2021) investigated the hydrophilic agent content of membranes single-soaked and cyclic NaOCl filtration at bench-scale and full-scale ageing in drinking water facilities and also reported no significant differences in hydrophilic agent removal [24]. However, the impacts of MBR operating conditions were not assessed in such ageing studies. While in direct filtration facilities, membranes are trapped inside their housing, in MBR modules, ZeeWeed® fibers are potted on both ends but not stretched under tension, thus being able to oscillate when aeration cycles are performed. These cycles occur every 10–30 s to detach foulants during filtration and cleaning protocols, by increasing shear stress at the membrane surface and convective forces. These operating conditions might also enhance hydrophilic agent dislodgement from the membrane structure.

Full-scale operation impacts on intrinsic permeability

Fibers harvested from a full-scale MBR seemed to experience an increasing Lp/Lp_0 for the whole study period, highlighting two main differences when compared to the sole hypochlorite action at bench scale: (i) permeability increased to a lesser extent and (ii) no decline in Lp/Lp_0 was experienced in the range studied. Both residual fouling and the differences in porosity changes can be related to these results.

For the first point, membranes operating at full scale still showed high amounts of PVP in the early stages, which was considered the main driver for permeability changes. Moreover, these membranes experience fouling, which is partially removed by chemical cleanings. However, the later appearance of bigger pores may enhance residual fouling in the long term as more organic matter is able to flow through and be adsorbed into the membranes (Figure 6). This may increase membrane hydrophobicity [22] and despite the increasing porosity, water is

hampered to flow through membranes, whereas membranes aged by single-soaking in NaOCl solution did not experience fouling, which enables the permeability to increase to higher values. By comparing the changes in permeability of membranes exposed only to sodium hypochlorite with membranes that went through cycles of a model fouling solution filtration and sodium hypochlorite cleaning at bench scale, Hajibabania et al. (2012) confirmed the smaller increases among the latter samples, assigning this difference to residual fouling [22]. In addition, the C × t value is used as a reference for comparison between these ageing methods, but it is worth noting that at full scale, NaOCl species are reacting not only with membrane polymers but also with the organic matter. In addition, plant operators reported declines in free chlorine concentrations of up to 30% over CIP soaking time. As the C × t in this study was calculated considering a stable free chlorine concentration over the CIP soaking time, this may have led to an overestimation of the actual C × t in direct contact to the membrane surface for full-scale samples. To avoid this probable overestimation in C × t for full-scale samples, the relationship between PVP content and Lp/Lp_0 is plotted in Figure 7 for both sets. For the same PVP removal, the increase in Lp/Lp_0 in samples aged at bench scale is higher than full-scale-aged membranes. This illustrates the role of the different pore size distributions and residual fouling, which impairs the increase in Lp/Lp_0, limiting the overestimation of exposure dose among full-scale samples.

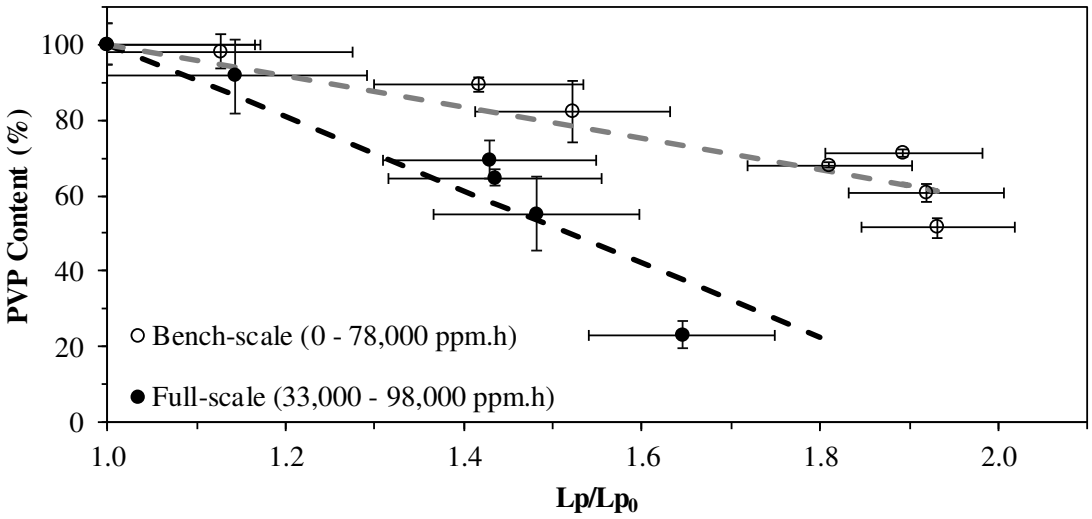

Figure 7: Relationship between PVP content removal and the changes in Lp/Lp0 for membranes aged at bench scale and at full scale.

For the second point, the lack of a permeability-declining phase might be linked to the cyclical backwashes that are known to increase pore size, contributing for a permeability increase [34]. In addition, a difference in the ageing process might also play a role. At bench scale, PVP was degraded until its content reached approximately 40% of the pristine fibers (Figure 5), but these molecules seemed not to be fully dislodged from the polymer structure (Figure 4.B), leading to the appearance of only smaller pores (Figure *6*). On the other hand, samples of full-scale-aged membranes continued to lose PVP, reaching 25% of the pristine membrane (Figure 5). This change along with the FTIR spectra in the PVP and its degradation product region (Figure 4.C) might indicate that PVP is not only degraded but also dislodged from the membrane structure, leading to the appearance of bigger pores as presented in Figure 6. The relationships between (i) PVP content and total pore volume (r = -0.864, p = 0.026, Pearson's test), (ii) total pore volume and Lp/Lp_0 (r = 0.904, p = 0.014, Pearson's test), and (iii) the direct relationship between PVP content and Lp/Lp_0 (r = -0.930, p = 0.007, Pearson's test) were confirmed to be statistically significant. These results highlight the importance of

the hydrophilic agent content in preserving the membrane filtration properties. Moreover, they illustrate that changes in Lp/Lp_0 are mostly governed by changes in pore size for either bench-scale or full-scale ageing.

Impacts of full-scale operation on cleaning recovery

The lower overall values of cleaning recovery for full-scale-aged membranes and its declining trend (Figure 3) can be ascribed to: (i) stronger interactions between foulants in mixed liquor and residual fouling remaining on the membrane surface; (ii) SEM images (supplementary material – Figure S. 2) showed a much rougher surface, which enhances fouling adsorption [11]; (iii) and the appearance of larger pores that can lead to higher amounts of matter inside the pores causing more severe pore clogging, which is a less reversible form of fouling than floc adhesion or cake formation [35]. In this study, pore size might contribute to cleaning recovery. However, statistical analysis were performed for changes in bigger pore volumes (>40 nm) and smaller pore volumes (<20 nm), separately, and no significant linear correlations were found ($p > 0.05$).

Ultimately, changes in cleaning recovery correlated well with the loss of hydrophilic agent and with the increase in Lp/Lp_0 ($r = 0.819$, $p = 0.046$ and $r = -0.897$, $p = 0.015$, Pearson's test, respectively). Since permeability correlated well with all other parameters, MBR operators should apply these measurements after CIP as an in situ diagnostic tool for membrane ageing. For increasing values, operators should expect a build-up of hydraulic irreversible fouling, which would lead to an increasing requirement for chemical cleanings. For future studies, this parameter may be correlated with full-scale filtration capacity data in order to identify the period when filtration is no longer possible, leading to membrane replacement. In addition, hydrophilic agent degradation seems to be the primary cause for all the other changes and as

in situ FTIR measurements are becoming available, it can also provide important information on membrane ageing in MBR operation.

5. Conclusions

The main conclusions of this study can be summarized as:

- Differences in the membrane ageing process for membranes aged by single soaking in NaOCl solution and during a 7-year period in an MBR treating municipal wastewater are highlighted by applying the same methodological protocol. A non-negligible contribution of filtration conditions, mechanical stress due to aeration, and residual fouling, specific to full-scale operating conditions, may significantly change ageing mechanisms. This study showed that understanding the mechanisms behind the action of NaOCl on PVDF membranes may not represent what actually occurs at full-scale operation and does not replace continuous autopsies of harvested fibers over the years.
- At bench scale, NaOCl species caused PVP oxidation, which led to the formation of small pores causing an increase in Lp/Lp_0 in contrast to the generally accepted hypothesis of pore enlargement reported in the literature. For exposures higher than 78,000 ppm.h, the membrane structure collapsed and Lp/Lp_0 decreased.
- In contrast to bench-scale ageing, full-scale-aged membranes experienced a decline in mechanical resistance due to MBR operating conditions, i.e., aeration. In addition, bigger pores are formed as a result of a more pronounced degradation of PVP when compared to bench-scale ageing, which ultimately led to an increasing Lp/Lp_0 during the study period.
- The increase in Lp/Lp_0 with age in full-scale samples is less intense than in bench-scale samples for the same PVP removal as a result of residual fouling on the membrane surface that also led to a decline in hydraulic cleaning recovery.

- Lp/Lp_0 and PVP content correlated well with all ageing changes among full-scale samples and can be applied for full-scale MBR operators as nondestructive in situ tools to monitor membrane ageing.
- Since the major changes seemed to be related to PVP oxidation, efforts are needed to change membrane formulations in order to achieve a stronger bond between PVP or other hydrophilic agents and the main polymer.
- Since bench-scale ageing protocols are not fully representative of full-scale MBR ageing, an accelerated ageing protocol at pilot-scale would be useful for validating long-term membrane performance.
- Changes in membrane properties from full-scale MBR are becoming available. Thus, efforts into membrane ageing modelling are needed to perform predictive calculations of the long-term ageing effects in MBR operation.

CRediT AUTHOR STATEMENT

Oliveira Filho Marcos: Conceptualization, Methodology, Visualization, Validation, Formal analysis, Investigation, Writing – Original Draft. Mailler Romain: Conceptualization, Validation, Supervision, Project administration, Writing – Review & Editing. Rocher Vincent: Conceptualization, Resources, Funding acquisition. Fayolle Yannick: Conceptualization, Validation, Supervision, Writing – Review & Editing. Causserand Christel: Conceptualization, Resources, Methodology, Validation, Supervision, Funding acquisition, Writing – Review & Editing.

ACKNOWLEDGMENTS

The authors would like to acknowledge Céline Briand, Julien Pouillaude (DI-SIAAP), and the DLE team (SIAAP) for their participation in mixed liquor analysis, membrane sampling, and

characterization. The technical contribution of Estelle Langlet and Ophélie Michot and their team (SEM-SIAAP) was also essential for this work. We are also grateful to Gwenaelle Guitier and Emma Roubaud (LGC-Toulouse) for their readiness to meet special membrane characterization demands.

FUNDING SOURCES

This research did not receive any specific grant from funding agencies in the public, commercial, or not-for-profit sectors.

REFERENCES

[1] The MBR site, (2021). https://www.thembrsite.com/ (accessed April 20, 2021).

[2] P. Krzeminski, L. Leverette, S. Malamis, E. Katsou, Membrane bioreactors – A review on recent developments in energy reduction, fouling control, novel configurations, LCA and market prospects, J. Membr. Sci. 527 (2017) 207–227. https://doi.org/10.1016/j.memsci.2016.12.010.

[3] G. Bertanza, M. Canato, G. Laera, M. Vaccari, M. Svanström, S. Heimersson, A comparison between two full-scale MBR and CAS municipal wastewater treatment plants: techno-economic-environmental assessment, Environ. Sci. Pollut. Res. 24 (2017) 17383–17393. https://doi.org/10.1007/s11356-017-9409-3.

[4] M. Bagheri, S.A. Mirbagheri, Critical review of fouling mitigation strategies in membrane bioreactors treating water and wastewater, Bioresour. Technol. 258 (2018) 318–334. https://doi.org/10.1016/j.biortech.2018.03.026.

[5] A. Fenu, W. De Wilde, M. Gaertner, M. Weemaes, G. de Gueldre, B. Van De Steene, Elaborating the membrane life concept in a full scale hollow-fibers MBR, J. Membr. Sci. 421–422 (2012) 349–354. https://doi.org/10.1016/j.memsci.2012.08.001.

[6] B. Verrecht, T. Maere, I. Nopens, C. Brepols, S. Judd, The cost of a large-scale hollow fibre MBR, Water Res. 44 (2010) 5274–5283. https://doi.org/10.1016/j.watres.2010.06.054.

[7] S. Robinson, S.Z. Abdullah, P. Bérubé, P. Le-Clech, Ageing of membranes for water treatment: Linking changes to performance, J. Membr. Sci. 503 (2016) 177–187. https://doi.org/10.1016/j.memsci.2015.12.033.

[8] S.Z. Abdullah, P.R. Bérubé, Filtration and cleaning performances of PVDF membranes aged with exposure to sodium hypochlorite, Sep. Purif. Technol. 195 (2018) 253–259. https://doi.org/10.1016/j.seppur.2017.12.004.

[9] S.Z. Abdullah, P.R. Bérubé, Assessing the effects of sodium hypochlorite exposure on the characteristics of PVDF based membranes, Water Res. 47 (2013) 5392–5399. https://doi.org/10.1016/j.watres.2013.06.018.

[10] F. Gao, J. Wang, H. Zhang, M.A. Hang, Z. Cui, G. Yang, Interaction energy and competitive adsorption evaluation of different NOM fractions on aged membrane surfaces, J. Membr. Sci. 542 (2017) 195–207. https://doi.org/10.1016/j.memsci.2017.08.020.

[11] I. Levitsky, A. Duek, E. Arkhangelsky, D. Pinchev, T. Kadoshian, H. Shetrit, R. Naim, V. Gitis, Understanding the oxidative cleaning of UF membranes, J. Membr. Sci. 377 (2011) 206–213. https://doi.org/10.1016/j.memsci.2011.04.046.

[12] K. Li, Q. Su, S. Li, G. Wen, T. Huang, Aging of PVDF and PES ultrafiltration membranes by sodium hypochlorite: Effect of solution pH, J. Environ. Sci. 104 (2021) 444–455. https://doi.org/10.1016/j.jes.2020.12.020.

[13] V. Puspitasari, A. Granville, P. Le-Clech, V. Chen, Cleaning and ageing effect of sodium hypochlorite on polyvinylidene fluoride (PVDF) membrane, Sep. Purif. Technol. 72 (2010) 301–308. https://doi.org/10.1016/j.seppur.2010.03.001.

[14] M.F. Rabuni, N.M.N. Sulaiman, N.A. Hashim, A systematic assessment method for the investigation of the PVDF membrane stability, Desalination Water Treat. 57 (2016) 1–12. https://doi.org/10.1080/19443994.2015.1012336.

[15] M.F. Rabuni, N.M. Nik Sulaiman, M.K. Aroua, C. Yern Chee, N. Awanis Hashim, Impact of in situ physical and chemical cleaning on PVDF membrane properties and performances, Chem. Eng. Sci. 122 (2015) 426–435. https://doi.org/10.1016/j.ces.2014.09.053.

[16] J. Ravereau, A. Fabre, A. Brehant, R. Bonnard, C. Sollogoub, J. Verdu, Ageing of polyvinylidene fluoride hollow fiber membranes in sodium hypochlorite solutions, J. Membr. Sci. 505 (2016) 174–184. https://doi.org/10.1016/j.memsci.2015.12.063.

[17] L. Ren, S. Yu, H. Yang, L. Li, L. Cai, Q. Xia, Z. Shi, G. Liu, Chemical cleaning reagent of sodium hypochlorite eroding polyvinylidene fluoride ultrafiltration membranes: Aging pathway, performance decay and molecular mechanism, J. Membr. Sci. 625 (2021) 119141. https://doi.org/10.1016/j.memsci.2021.119141.

[18] L. Vanysacker, R. Bernshtein, I.F.J. Vankelecom, Effect of chemical cleaning and membrane aging on membrane biofouling using model organisms with increasing complexity, J. Membr. Sci. 457 (2014) 19–28. https://doi.org/10.1016/j.memsci.2014.01.015.

[19] Q. Wang, H. Zeng, Z. Wu, J. Cao, Impact of sodium hypochlorite cleaning on the surface properties and performance of PVDF membranes, Appl. Surf. Sci. 428 (2018) 289–295. https://doi.org/10.1016/j.apsusc.2017.09.056.

[20] Q. Wu, X. Zhang, G. Cao, Impacts of sodium hydroxide and sodium hypochlorite aging on polyvinylidene fluoride membranes fabricated with different methods, J. Environ. Sci. 67 (2018) 294–308. https://doi.org/10.1016/j.jes.2017.07.014.

[21] Y. Zhang, J. Wang, F. Gao, Y. Chen, H. Zhang, A comparison study: The different impacts of sodium hypochlorite on PVDF and PSF ultrafiltration (UF) membranes, Water Res. 109 (2017) 227–236. https://doi.org/10.1016/j.watres.2016.11.022.

[22] S. Hajibabania, A. Antony, G. Leslie, P. Le-Clech, Relative impact of fouling and cleaning on PVDF membrane hydraulic performances, Sep. Purif. Technol. 90 (2012) 204–212. https://doi.org/10.1016/j.seppur.2012.03.001.

[23] F. Gao, J. Wang, H. Zhang, Y. Zhang, M.A. Hang, Effects of sodium hypochlorite on structural/surface characteristics, filtration performance and fouling behaviors of PVDF membranes, J. Membr. Sci. 519 (2016) 22–31. https://doi.org/10.1016/j.memsci.2016.07.024.

[24] S.J. Robinson, P.R. Bérubé, Seeking realistic membrane ageing at bench-scale, J. Membr. Sci. 618 (2021) 118606. https://doi.org/10.1016/j.memsci.2020.118606.

[25] S. Robinson, P.R. Bérubé, Membrane ageing in full-scale water treatment plants, Water Res. 169 (2020) 115212. https://doi.org/10.1016/j.watres.2019.115212.

[26] H. Yu, X. Li, H. Chang, Z. Zhou, T. Zhang, Y. Yang, G. Li, H. Ji, C. Cai, H. Liang, Performance of hollow fiber ultrafiltration membrane in a full-scale drinking water treatment plant in China: A systematic evaluation during 7-year operation, J. Membr. Sci. 613 (2020) 118469. https://doi.org/10.1016/j.memsci.2020.118469.

[27] B. Pellegrin, R. Prulho, A. Rivaton, S. Thérias, J.-L. Gardette, E. Gaudichet-Maurin, C. Causserand, Multi-scale analysis of hypochlorite induced PES/PVP ultrafiltration membranes degradation, J. Membr. Sci. 447 (2013) 287–296. https://doi.org/10.1016/j.memsci.2013.07.026.

[28] R. Prulho, S. Therias, A. Rivaton, J.-L. Gardette, Ageing of polyethersulfone/polyvinylpyrrolidone blends in contact with bleach water, Polym.

Degrad. Stab. 98 (2013) 1164–1172. https://doi.org/10.1016/j.polymdegradstab.2013.03.011.

[29] E.P. Barrett, L.G. Joyner, P.P. Halenda, The Determination of Pore Volume and Area Distributions in Porous Substances. I. Computations from Nitrogen Isotherms, J. Am. Chem. Soc. 73 (1951) 373–380. https://doi.org/10.1021/ja01145a126.

[30] R Core Team, R: A Language and Environment for Statistical Computing, R Foundation for Statistical Computing, Vienna, Austria, 2019.

[31] B.A. Pulido, O.S. Habboub, S.L. Aristizabal, G. Szekely, S.P. Nunes, Recycled Poly(ethylene terephthalate) for High Temperature Solvent Resistant Membranes, ACS Appl. Polym. Mater. 1 (2019) 2379–2387. https://doi.org/10.1021/acsapm.9b00493.

[32] G. Matar, G. Gonzalez-Gil, H. Maab, S. Nunes, P. Le-Clech, J. Vrouwenvelder, P.E. Saikaly, Temporal changes in extracellular polymeric substances on hydrophobic and hydrophilic membrane surfaces in a submerged membrane bioreactor, Water Res. 95 (2016) 27–38. https://doi.org/10.1016/j.watres.2016.02.064.

[33] C. Causserand, B. Pellegrin, J.-C. Rouch, Effects of sodium hypochlorite exposure mode on PES/PVP ultrafiltration membrane degradation, Water Res. 85 (2015) 316–326. https://doi.org/10.1016/j.watres.2015.08.028.

[34] E. Akhondi, F. Zamani, A. W.K. Law, W.B. Krantz, A. G. Fane, J. Wei Chew, Influence of backwashing on the pore size of hollow fiber ultrafiltration membranes, J. Membr. Sci. (521) 2017 33-42. https://doi.org/10.1016/j.memsci.2016.08.070

[35] H. Lin, M. Zhang, F. Wang, F. Meng, B.-Q. Liao, H. Hong, J. Chen, W. Gao, A critical review of extracellular polymeric substances (EPSs) in membrane bioreactors: Characteristics, roles in membrane fouling and control strategies, J. Membr. Sci. 460 (2014) 110–125. https://doi.org/10.1016/j.memsci.2014.02.034.

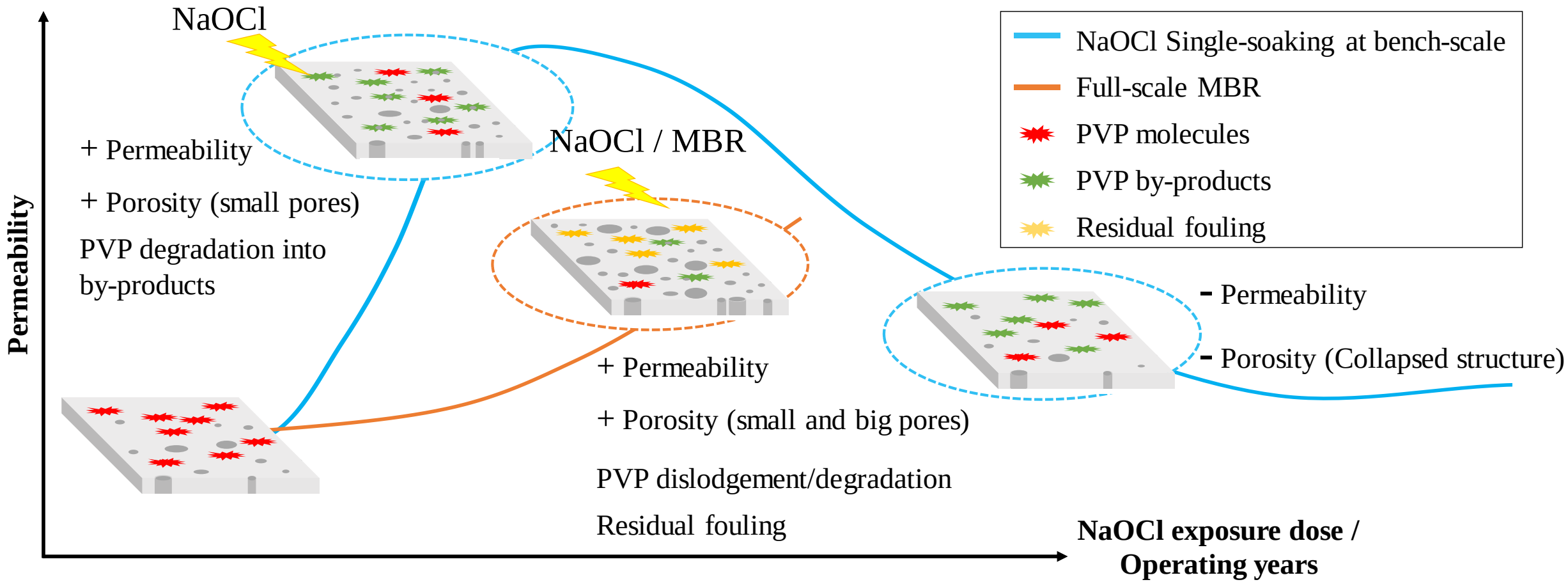
NaOCl
+ Permeability
+ Porosity (small pores)
PVP degradation into by-products
NaOCl / MBR
+ Permeability
+ Porosity (small and big pores)
PVP dislodgement/degradation
Residual fouling
- Permeability
- Porosity (Collapsed structure)
NaOCl Single-soaking at bench-scale
Full-scale MBR
PVP molecules
PVP by-products
Residual fouling
Permeability
NaOCl exposure dose / Operating years